Time-Dependent Behavior of the 10830 Å Line in a Low-Pressure Helium Afterglow*

C. B. Collins and W. B. Hurt

Southwest Center for Advanced Studies, Dallas, Texas 75230

(Received 10 October 1968)

The time-dependent behavior of the intensity of the 10 830 Å line emitted from a pulsed helium afterglow at 3 Torr has been investigated with an improved spectrometric system of sufficient sensitivity-bandwidth ratio to resolve the behavior of this line over a 50-msec time interval. A high degree of correlation was observed between the 10 830 Å line intensity and the 4650 Å molecular-band intensity for afterglow times in excess of 2 msec. A recombination of the He_2^+ ion leading to dissociation and having a rate coefficient of $2 \times 10^{-11} cm^3/sec$ at 10^{12} electrons/cm^3 is consistent with data.

INTRODUCTION

The origin of the 10 830 Å line $(2^3P \to 2^3S)$ in the helium afterglow has been the subject of some controversy for the past few years. Collins and Robertson[1] first reported a study of this transition in a flowing-helium afterglow[2] in which a marked similarity was observed between the dependence on afterglow parameters of the intensity of this line and the intensity of the helium molecular-band radiation as typified by the band at 4650 Å $(3^3\Pi_g \to 2^3\Sigma_u^+)$. As recognized at the time[3,4] this was in contrast to the behavior of the visible atomic light which showed no such correlation with the molecular light.

This anomalous dependence of the 10 830 Å line on afterglow parameters was not confirmed in later work on other helium afterglow systems. On the contrary, subsequent theoretical and experimental results have raised concern that perhaps these early results reflected some extrinsic properties of the system rather than the recombination processes themselves. In particular, recent measurements[5-7] of the time-dependent behavior of the atomic light emitted in the visible wavelength range from low-pressure helium afterglows have shown the principal source of this visible light to be two-electron collisional-radiative recombination[8] of He^+ with electrons. Although the studies did not report measurement of the 10 830 Å line, it can be reasonably inferred from them that a substantial intensity for this line must be expected as a result of collisional-radiative recombination of He^+. This contribution to the total intensity of the 10 830 Å line would be consequently uncorrelated with the emission of the molecular light which apparently results from the recombination of the molecular ion[9] He_2^+. Born[10] has recently reported this uncorrelated component to be the only contribution to the 10 830 Å line intensity in a pulsed helium afterglow at very early times, $t < 2$ msec,

and for electron densities of the order of $10^{13} cm^{-3}$. He attributed a transient correlation of the 10 830 Å line and 4650 Å band to a fortuitous modification of the functional form by the time-dependent 2^3S metastable absorption of the 10 830 Å line. In addition the suggestion was made that perhaps the uncorrelated component was similarly modified by the varying degree of self absorption of the 10 830 Å line in the earlier work of Collins and Robertson and that in fact no necessarily correlated component of the 10 830 Å intensity existed.

Mulliken's[11] recent theoretical analysis of the potential energy curves of the excited states of He_2 further strengthened this argument by revealing the absence of any purely repulsive states from which He_2 could dissociate into an atomic state capable of yielding the emission of a 10 830 Å photon either directly or as the result of subsequent cascading. Consequently, if Born's results could be confirmed and extended to later times and a wider range of the afterglow parameters, a rather consistent model of the helium afterglow would be established in which molecular ions recombine only into molecular states and atomic ions undergo collisional-radiative recombination to yield all observed atomic light during the afterglow period. Conversely, a confirmation of the early Collins and Robertson results in a different system would pose a substantial problem in analysis.

This paper reports such a study of the 10 830 Å emission from a pulsed helium afterglow at a pressure chosen to be 3 Torr to insure appreciable concentrations of both atomic and molecular helium ions. The afterglow period under observation was 50 msec with electron densities in the 10^{11}–10^{12} cm^{-3} range.

APPARATUS AND TECHNIQUES

The afterglow cell, gas handling system, and

operational cycle have been discussed elsewhere,[5] and were employed essentially without change in this experiment. Visible radiation from the afterglow was spectroscopically analyzed with a 0.5-m Ebert monochromator with sets of slits to give 1.6 Å and 4.0 Å resolution, as needed.

Dependable measurement of the 10 830 Å intensity in pulsed helium afterglows is particularly difficult, primarily as a consequence of the low sensitivity of available S-1 photomultipliers in this region. In addition, an abundance of spectral features in second and third order, together with possible grating ghosts, coincide with the first-order 10 830 Å line. This necessitates substantial preliminary filtering, further reducing available intensity. Several combinations of filters and spectrometer slits were tried in order to maximize the sensitivity-bandwidth ratio. Three were found to give identical forms of intensity as a function of time, but with differing probable errors. Two of these were slits to give 16 Å resolution in the first order together with prefiltering either by Corning 2550 glass or by an interference filter with 100 Å bandwidth centered at 10 830 Å and having higher orders suppressed. The third system gave the highest sensitivity and used the openings in the spectrometer slit block with prefiltering by the interference filter.

Output pulses from the photomultiplier were conditioned with a 10-MHz pulse-counting system and continuously accumulated in successive phase increments of width controlled by an on-line programmable data-acquisition system as discussed previously.[12] Operation for times sufficiently long to provide acceptable statistics necessitated the use of real-time sieving of data collected during each phase increment. In practice, the system was programmed to halt if the accumulated counts in any frame for a single cycle deviated from the previous cycles by an amount in excess of that statistically expected. All runs which were abnormally terminated in this manner were rejected. As a consequence of the relatively poor electrical shielding of the infrared-sensitive photomultiplier necessitated by the cooling technique employed, not more than 100 000 cycles of data could be accumulated by phase for the 10 830 Å line. Visible lines were measured for periods of the order of 500 000 cycles.

All spectroscopic data was subsequently analyzed on a digital computer according to standard statistical procedures. Probable errors were calculated from the standard deviation of the data and base line.

RESULTS

From an examination of the spectroscopic data, it was found that the time-dependent behavior of the 10 830 Å helium atomic line was in fact closely

similar to the behavior of the helium molecular light as typified by the band at 4650 Å under these experimental conditions for all afterglow times greater than about 2 msec. Conversely, the time-dependent behavior of the 10 830 Å line was quite dissimilar to the behavior of all other helium atomic lines[13] observed over the range of afterglow times greater than about 2 msec.

Figure 1 is typical of this data and illustrates the time dependence of the 10 830 Å $(2^3P \rightarrow 2^3S)$ transition and the 4471 Å $(4^3D \rightarrow 2^3P)$ transition of atomic helium together with the 4650 Å $(3^3\Pi_g \rightarrow 2^3\Sigma_u^+)$ helium molecular band. No data was obtained for the first 600 μsec during which the power pulse occurred. Intensities during the afterglow period have been presented in terms of detected photon count rates. Horizontal and vertical dimensions indicate, respectively, the uncertainty in time caused by the finite width of the phase increment and the statistical nature of the data. Where possible, the intensity has been plotted together with limits representing the data
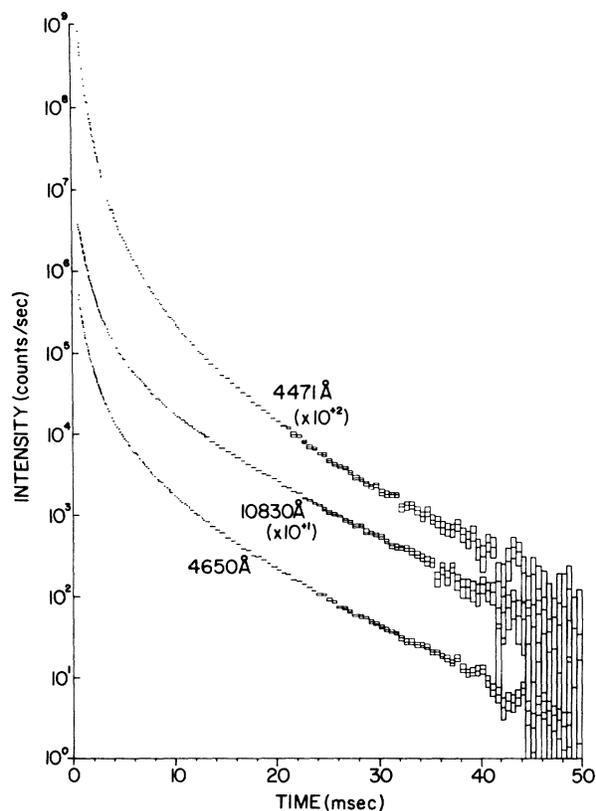
FIG. 1. A graph of the afterglow intensity of the 4650 Å $(3^3\Pi \rightarrow 2^3\Sigma)$ molecular band as a function of time, together with the intensities of the 10 830 Å $(2^3P \rightarrow 2^3S)$ and 4471 Å $(4^3D \rightarrow 2^3P)$ atomic lines increased one and two decades respectively for separation. At late times, limits representing data ±one standard deviation are shown.

± one standard deviation. In instances of detected intensities sufficiently small compared to the "dark current" count rate, a finite probability exists for measuring a negative difference in data-count rate and dark-current rate. Such points plot at $-\infty$ in the presently employed analysis scheme, and have been deleted from the figure for clarity.

Graphs of the primary data, such as Fig. 1, which must span many orders of magnitude do not emphasize the degree of similarity or dissimilarity of the functional dependences on time. More useful for comparisons is the normalized fractional difference f, where

$$f = (I_1 - CI_2)/(I_1 + CI_2) \ , \tag{1}$$

I_1 and I_2 represent the instantaneous intensities of the two spectral features to be compared, and C is a normalizing constant generally chosen so that

$$\lim_{t \to \infty} f = 0 \tag{2}$$

Where possible, values of f can be plotted as a function of time together with limits representing the data ± one standard deviation σ_f, the latter being approximated

$$\sigma_f = (I_1 + CI_2)^{-1}(1 + f^2)^{1/2}\sigma \ , \tag{3}$$

whenever $|\sigma_f| < |f|$,   (4)

where σ represents a standard deviation of $(I_1 + CI_2)$. Otherwise σ_f can be determined less conveniently from the joint distribution of $(I_1 - CI_2)$ and $(I_1 + CI_2)$ integrated over the appropriate region of the variate space according to standard statistical techniques.

Figures 2(a) and 2(b) present the normalized fractional differences between the intensities of the 4650 Å band and 10 830 Å line and the intensities of the 4471 Å and 10 830 Å lines, respectively, emitted axially from the cell and consequently subject to the greatest degree of self-absorption. Figure 3 presents the normalized fractional differences between the intensities of the 4650 Å band and 10 830 Å line emitted radially from the cell and subject to the least degree of self-absorption.

From Figs. 2(a) and 3, it can be seen that the functional form of the dependence of the intensity of the 10 830 Å line on afterglow time differs from that of the intensity of the 4650 Å band in both the axial and radial measurements by less than 10% at all times greater than about 2.0 msec. Figure 2b shows that the dissimilarity between the intensity of a typical visible atomic line such as 4471 Å and the 10 830 Å line is significantly greater than 10% for all times less than 25 msec for
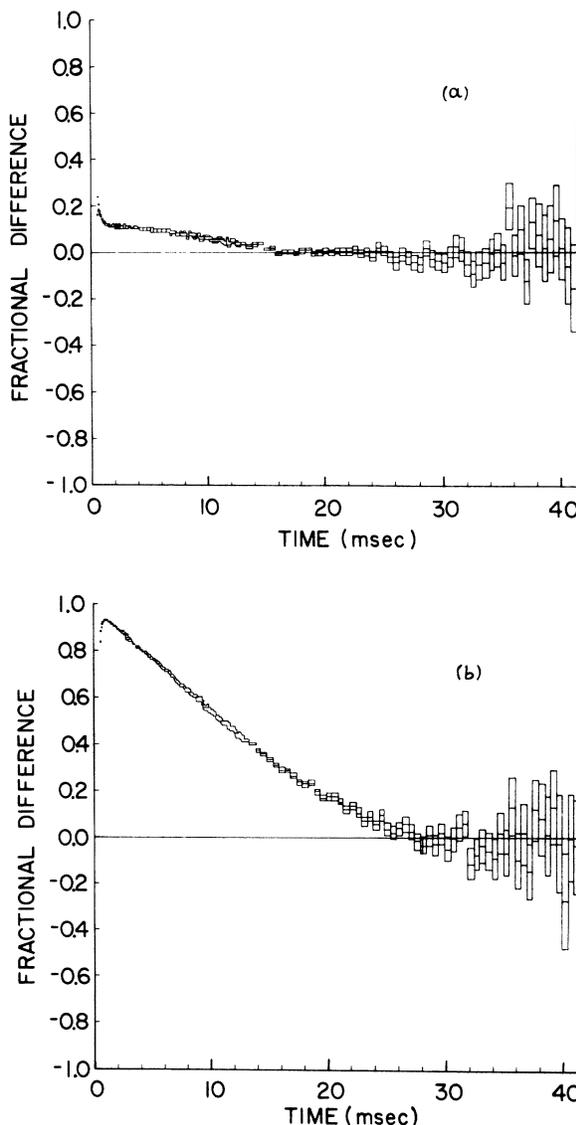
FIG. 2. Graphs of the normalized fractional difference in the intensities emitted axially from the afterglow of pairs of spectral features as functions of time. Limits representing data ±one standard deviation are shown where possible. (a) Intensity difference of the 10 830 Å line and the 4650 Å band. (b) Intensity difference of the 10 830 and 4471 Å lines.

light emitted axially. The same degree of dissimilarity appeared in the corresponding radial measurement.

The apparently close parallelism of the 10 830 Å and molecular light at all times immediately suggests that the intensity should be examined as a continuous function of wavelength at these times to determine whether the behavior of the 10 830 Å
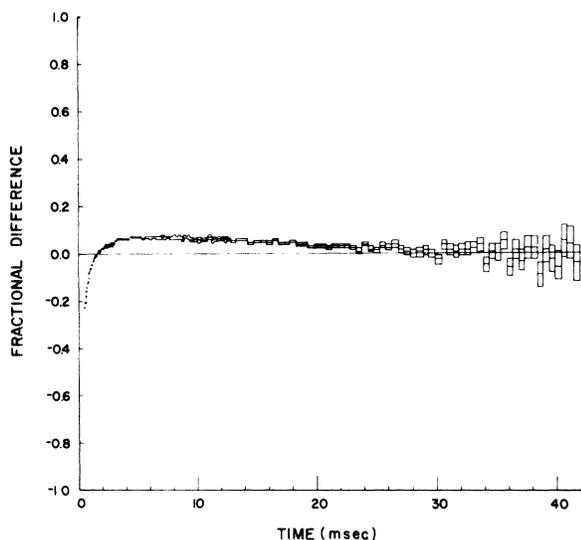
FIG. 3. A graph of the normalized fractional differ-
ence in the intensities emitted radially from the after-
glow of the 10 830 Å line and the 4650 Å band as a
function of time. Limits representing data ±one stan-
dard deviation are shown where possible.

line can be attributed to a combination of near-
lying and scattered molecular light as found by
Niles[5] in the visible region in a system of consid-
erably lower resolution. Figure 4 presents the
spectrum of a 24 Å interval about 10 830 Å inte-
grated over the 4-msec time interval centered on
15 msec. As in Fig. 1, the average detected-
photon count rate is plotted vertically together with
the statistically expected values of data ± one stan-
dard deviation. The observed profile, within the
probable error limits, is identical to the profile
at all earlier times. Data at successively later
times also supports a time-independent spectral
distribution of the photon count rate near 10 830 Å.
Consequently, it appears valid to assume that the
behavior illustrated in Figures 1, 2, and 3 does in
fact represent the functional dependence of the
10 830 Å atomic line at all afterglow times spanned
by the measurements.

The dependence of the 10 830 Å light on electron
temperature was examined in a qualitative way by
heating the free electrons with a recurrent micro-
wave pulse synchronized with the basic afterglow
cycle. In this particular case, a framing pattern
was employed by the acquisition system which en-
abled resolution of several phase increments of
data during the 200-μsec period in which the 2.4-
GHz heating pulse was on. At low applied powers,
the intensity of both the 10 830 Å and molecular
light was found to decrease by equal fractions for
the duration of the power pulse. With increasing
power levels, the intensities were found to de-

crease by progressively larger amounts, the
10 830 Å light generally following the quenching
pattern of the molecular rather than the visible
atomic light.[12] No attempt at quantitative presen-
tation of the quenching data has been attempted
since no provisions were made to measure either
instantaneous electron temperatures or micro-
wave field intensities in the plasma.

Final calibration of the spectrometric system at
10 830 Å was performed against a standard of
radiance traceable to NBS. The calibration point
was chosen to be 1 msec at which time the 2^3P
population was determined from the measured ab-
solute 10 830 Å intensity to be 1.5×10^7 cm^{-3}.

ANALYSIS AND CONCLUSIONS

The qualitative aspects of the strong inverse de-
pendence of light on microwave heating at low
microwave powers in the absence of a similar de-
pendence of atomic metastable concentration[13]
presents compelling evidence for a recombination
origin of the ambient 10 830 Å intensity at all
times observed. This is consistent with the re-
combination origin of the other afterglow lines,
molecular as well as atomic.
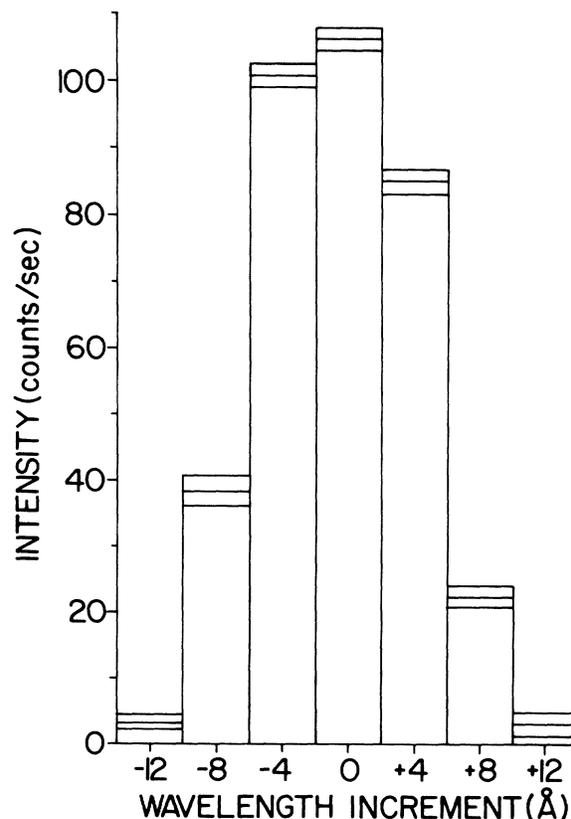
FIG. 4. A graph of intensity as a function of wave-
length of the 24 Å interval centered on 10 830 Å integrated
over the 4-msec time interval centered on 15 msec.
Data together with limits representing ±one standard
deviation are shown.

Of particular interest are the exponential decay constants of the various lines compared. Table I presents decay constants which have been obtained from a least-squares fit of the logarithm of the data to a trial line in terms of the deviation between it and the data in units of standard deviation of the data. In this manner decay constants were obtained for the 10-msec time interval centered on 20 msec. A measure of the error in the form of the standard deviation of the least squares fit is also shown in Table I.

The agreement in decay constants between the 10 830 Å line and the 4650 Å molecular band further amplify the similarity in functional forms displayed in Figs. 2(a) and 3. The dissimilarity in decay constants for the 10 830 Å and 4471 Å lines is to be expected as a consequence of the large fractional differences found in Fig. 2(b).

It appears that the basic observation of Ref. 1 is confirmed in that the time-dependent behavior of the observed intensities of the 10 830 Å atomic line and the 4650 Å molecular band are highly correlated for a significant fraction of the afterglow period. This does not necessarily imply that the population of the 2^3P level follows the 10 830 Å intensity, since, as suggested by Born,[10] the radiation is to some extent trapped by the relatively large time-dependent concentration of lower-state 2^3S atoms. Nevertheless, the 2^3P state can radiate only at 10 830 Å, and all such photons initially emitted by the ambient 2^3P population must ultimately exit from the afterglow, provided the probability of nonradiative de-excitation of the 2^3P states subsequently formed by the sequence of reabsorptions of the initial photons is sufficiently small.

The most probable types of nonradiative de-excitation under the conditions of this experiment appear to be the following

$$He(2^3P) + e \rightarrow He(2^3S) + e \qquad (5)$$

and $\quad He(2^3P) + e \rightarrow He(2^1S) + e \ . \qquad (6)$
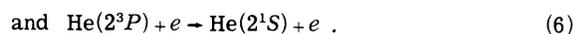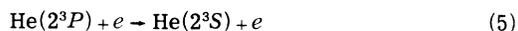
Classical Gryzinski-type calculations[14] of the rates expected for these processes suggest a value not in excess of 10^{-8} cm^3/sec for the total nonradiative de-excitation rate, although the accuracy of such calculations is in question when applied to different angular momentum states of the same principle quantum number. Nevertheless, even at the early times, ~ 3 msec, values of electron density are sufficient to give a superelastic de-excitation rate only of the order of 10^4 sec^{-1}, a value three orders of magnitude less than the natural radiative rate. "Random walk" estimates based on measured 2^3S densities indicate less than 30 successive absorptions and emissions are

TABLE I. Experimental values of the exponential decay constants characteristic of the pertinent atomic and molecular lines together with the probable error.

Species	Decay constant (sec^{-1})	Standard deviation (sec^{-1})
He (4^3D)	235	2
He (2^3P)	174	2
He$_2$ ($3^3\Pi$)	175	2

necessary before the average photon can emerge along the greatest dimension of the plasma. Consequently it is most unlikely that a 10 830 Å photon initially emitted in the cell will fail to emerge from the afterglow.

In this case even rather severe self-absorption can serve only to introduce a time-dependent degree of anisotropy in the 10 830 Å intensity emitted from the cell, causing some of the intensity normally emitted along the greater pathlengths to appear along the shorter dimensions of the afterglow. The only other possibly confusing effect of self-absorption would be a delay in the release of the photons of such magnitude that the time scale of a trapped line could not be equated to that of a nontrapped line. However, such delays are of the order of the product of the lifetime of the upper state and the average number of successive absorptions. In this case under the worst conditions of axial radiation this amounts to an uncertainty in the time scale of 3 μsec which is substantially less than the uncertainty caused by the finite duration of the phase increments during which the light is sampled.

Solution of the trapped radiation problem[15] in sufficient detail to permit correction of the data for the time-dependent anisotropy caused by the self-absorption is exceeding by complex when applied to a system of this configuration and was not attempted. Rather, the importance of the anisotropy was bracketed by repeating all measurements so that the intensity was sampled along both the shortest and longest dimensions of the afterglow, so that any deficiency of intensity occurring in the latter would be detected as an increase in emission in the former measurement. Such an effect was detected but was entirely insufficient to account for the difference between the visible atomic lines as typified by the 4471 Å line and the 10 830 Å line. On the contrary, as illustrated in Figs. 2a and 3 the radial (short pathlength) data improved the correlation between the 4650 Å molecular emission and the 10 830 Å line.

It is therefore strongly indicated that the 2^3P population has a dependence on time closely correlated with that of the 4650 Å band under the conditions of this experiment for the major fraction of the afterglow period. This comprises

rather compelling evidence for the production of 2^3P atoms as the result of the recombination of the molecular ion He_2^+. As mentioned in the introduction, this poses a substantial problem in analysis in view of Mulliken's theoretical treatment[11] of He_2 in which no purely repulsive states were found. Possibly some multibody process can occur which results in the predissociation of one of the excited states of He_2 capable of dissociating into a 2^3P and a ground-state helium atom.

From a strictly phenomenological viewpoint a recombination rate for dissociation can be found for the process

$$He_2^+ + e + X \to \cdots \to He(2^3P) + He + X \quad , \qquad (7)$$
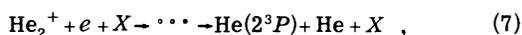
where the X represents a possible third body and the dots indicate the probability of intermediate steps. The gain of 2^3P atoms can be represented as

$$(d/dt)[2^3P] = \alpha_d(2^3P)[He_2^+][e] \quad , \qquad (8)$$

where $\alpha_d(2^3P)$ is the coefficient of recombination leading to dissociation into the 2^3P level. As discussed earlier this must approximately equal the rate at which 2^3P atoms are lost by spontaneous radiation. Applying this to the data of Fig. 1 yields the results presented in Table II. The lower limits on α_d are obtained from the product $\alpha_d(2^3P)[He_2^+]$ by assuming every He_2^+ ion can participate in reaction (7) regardless of state and

TABLE II. Deduced values of the rate for the production of 2^3P atoms, $\alpha_d(2^3P)[He_2^+]$, and the lower limit for the recombination rate coefficient α_d of electrons with He_2^+ leading to dissociation.

Electron density (cm^{-3})	$\alpha_d(2^3P)[He_2^+]$ (sec^{-1})	α_d, lower limit (cm^3/sec)
1×10^{12}	21	2.1×10^{-11}
3×10^{11}	3.7	1.2×10^{-11}
1×10^{11}	0.34	3.4×10^{-12}

further that the concentration of all other ions is negligible.

Viewed as a rate coefficient of the loss of charged species, α_d is a lower limit in a further sense in that it neglects the possible contribution of recombinations leading to dissociation directly into undetected or nonradiating states, principally the 2^1P, 2^1S, and 2^3S states. The data appears to indicate a dependence of α_d, and, moreover, of $\alpha_d(2^3P)[He_2^+]$, on electron density similar to that expected[16] from collisional-radiative recombination of He_2^+. The most probable process in general agreement with the data and Mulliken's potential curves is some form of neutral collision-induced dissociation of one or more excited states of He_2 resulting from the collisional-radiative recombination of He_2^+, although the predominance of such a process is surprising at this rather low neutral-gas pressure.

CONCLUSION

The data of this experiment serves to verify the originally reported strong phenomenological correlation between the 2^3P population and the intensity of helium molecular light observed in recombining helium afterglows at low neutral pressure and moderate electron density. The conflicting data of Born[10] have been neither confirmed nor refuted, since his measurements were confined to very early times and high electron densities, conditions under which the correlation was not pronounced in this experiment.

The detailed cause of the strong dependence of 2^3P population on the excited molecular population is obscure but in general appears to indicate the existence of a type of recombination of He_2^+ leading to dissociation with a rate coefficient of the order of 2×10^{-11} cm^3/sec at 10^{12} electrons/cm^3. Further work is needed to define the particular process by which the molecular systems dissociate.

ACKNOWLEDGMENT

[1]C. B. Collins and W. W. Robertson, Bull. Am. Phys. Soc. 10, 189 (1965).

[2]C. B. Collins and W. W. Robertson, J. Chem. Phys. 40, 701 (1964).

[3]W. W. Robertson, J. Chem. Phys. 42, 2064 (1965).

[4]C. B. Collins and W. W. Robertson, J. Chem. Phys. 43, 4188 (1965).

[5]C. B. Collins and W. B. Hurt, Phys. Rev. 167, 166 (1968).

[6]D. E. Kerr, Johns Hopkins University Report, 1960 (unpublished); C. S. Leffel, M. N. Hirsh, and D. E. Kerr, to be published.

[7]R. A. Gerber, G. F. Sauter, and H. J. Oskam, Physica 32, 2173 (1966).

[8]D. R. Bates, A. E. Kingston, and R. W. P. McWhirter, Proc. Roy. Soc. (London) A267, 297 (1962).

[9]C. B. Collins and W. W. Robertson, J. Chem. Phys. **40**, 2208 (1964).

[10]G. K. Born, Phys. Rev. **169**, 155 (1968).

[11]R. S. Mulliken, Phys. Rev. **136**, A962 (1964).

[12]C. B. Collins and W. B. Hurt, Phys. Rev. **177**, 257 (1969).

[13]The experimental conditions under which these

measurements were made were the same as those reported in Ref. 12, which discusses the behavior of the visible atomic emission, molecular band intensity, electron density, and metastable concentration.

[14]M. Gryzinski, Phys. Rev. **115**, 374 (1959).

[15]T. Holstein, Phys. Rev. **72**, 1212 (1947).

[16]C. B. Collins, Phys. Rev. **175**, 160 (1968).

Surface Tension at the He³-He⁴ Interface*

W. Brouwer†

Theoretical Physics Institute, Department of Physics, University of Alberta, Edmonton, Canada

and

R. K. Pathria

Department of Physics, Panjab University, Chandigarh, India

(Received 14 October 1968)

An estimate is made of the interfacial surface tension in a phase-separated mixture of He³-He⁴ on the basis of Atkins's approach. A corresponding experimental study should elucidate the role played by the vibrational surface modes of a quantum fluid.

According to Atkins[1] and Brouwer and Pathria[2] the surface tension $\sigma(T)$ of liquid helium II may be written as

$$\sigma(T) = \sigma_i(T) + \sigma_v[T, \sigma_i(T)] , \qquad (1)$$

where σ_i is the so-called "intrinsic" surface tension of the liquid that arises from the interatomic interactions, while σ_v is the contribution made by the quantized vibrational modes of the free surface. These vibrational modes are assumed to be similar in nature to the macroscopic capillary waves whose (frequency-dependent) phase velocity area v is given by the relationship

$$v = (2\pi\sigma/\lambda\rho)^{1/2} , \qquad (2)$$

ρ being the mass density of the liquid and λ the wavelength of the mode in question. In the spirit of the Debye theory of solids, one chooses a cut-off frequency ν_c such that the total number of normal modes of vibration in the surface becomes equal to the number of molecules in a monomolecular layer at the surface. One thereby finds that a significant part of the total surface energy of the liquid comes from the presence of these surface modes.

At absolute zero again, the surface tension of liquid helium consists of the intrinsic surface tension $\sigma_i(0)$ and the zero-point energy of the surface modes $\sigma_v(0)$. A theoretical estimate of $\sigma_i(0)$ has been made by Brouwer and Pathria[2] on the basis of the imperfect gas model of Gross[3] and Pitaevski,[4] where one calculates the energy associated with the nonuniformity that exists in the surface region of the liquid and identifies it with the intrinsic surface tension $\sigma_i(0)$. To obtain agreement with the experimental value[5] of $\sigma(0)$, viz. 0.37 erg cm⁻², one concludes that $\sigma_i(0) \approx 0.14$ erg cm⁻² and $\sigma_v(0) \approx 0.23$ erg cm⁻². The temperature-dependent part of $\sigma(T)$, on the other hand, is reasonably well explained by the free energy contribution arising from the ripplons alone, with the result[1,2]

$$\sigma(T) \approx \sigma(0) - aT^{7/3},$$

where $a = 6.5 \times 10^{-3}$ erg cm⁻² °K⁻⁷/³.

Subsequently, Lovejoy[6] pointed out that the experimental results on the surface tension of liquid He³ can be understood on the basis of the existence of surface modes of vibration. It then turns out that the experimentally extrapolated value $\sigma(0)$ of the zero-point surface tension of